Available online at www.sciencedirect.com
SCIENCE DIRECT®
Journal of Sound and Vibration 277 (2004) 353–367
JOURNAL OF SOUND AND VIBRATION
www.elsevier.com/locate/jsvi

Electroelastic vibrations and transformation ratio of a planar piezoceramic transformer

V.L. Karlash

S.P. Timoshenko Institute of Mechanics of the National Academy of Sciences of the Ukraine, Nesterov st. 3, 03057 Kyiv, Ukraine

Received 28 May 2002; accepted 11 September 2003

Abstract

Piezoelectric transformers of the transverse–longitudinal type are used in small-sized electronic devices, in which the traditional electromagnetic transformers are inapplicable. A monolithic piezoceramic rectangular plate, having two sections of transverse and longitudinal polarization with transformation of an electric voltage from input to output was described almost 50 years ago. The method of equivalent electric circuits was used to derive an approximate formula for the transformation ratio for no-load conditions without accounting for the difference between elastic compliance in different sections, which may be 10–15%.

In the author's previous papers, the forced vibrations of a classical transverse–longitudinal piezotransformer were analyzed. A more precise formula was derived for the transform ratio with regard to the difference between the elastic compliances in the input and output sections. It was established that the transforming ratio is inversely proportional to the squared frequency and is a good match with experimental data. It was shown that the longitudinal mechanical stresses in both sections of the transformer are axisymmetric with respect to the separating line.

In the present paper, the forced vibrations of a piezoelectric transformer of a transverse–longitudinal type are considered with respect to dependence of the transformer parameters upon the difference of the elastic compliances in different sections. Experimental data are also considered. The complex function method is applied for numerical analysis. Amplitude–frequency characteristics of the piezotransformer are compared with those for a thin piezoceramic rectangular plate.

1. Introduction

The forced electroelastic vibrations of a planar piezoelectric transformer with different sections of transverse–longitudinal polarizations are considered. The use of piezoelectric transformers of

E-mail address: elektr@inmech.kiev.ua (V.L. Karlash).

0022-460X/$ - see front matter
doi:10.1016/j.jsv.2003.03.012

different geometrical shapes is well known. An idea of double transformation of an electric energy into mechanical energy and back by means of the monolithic piezoceramic plate was first proposed almost 50 years ago by Rosen [1]. His device was made from Barium Titanate piezoceramics as a thin rectangular plate having sections of transverse and longitudinal polarization. In Ref. [2] a method of equivalent electric circuits was used to derive an approximate formula for the transformation ratio for both no-load and maximum output power conditions without accounting for the difference between the elastic compliances in different sections, which may be 10–15%. Extensive experimental data for Rosen-type transformer structures of various piezoceramic compositions are presented in Refs. [3,4], where the first resonance was mainly considered. Radial vibrations of thin piezoceramic discs were described in Refs. [5,6]. Such devices may be used in current transformers and in frequency filters.

A piezoelectric transformer for AC–DC converters with a multilayered construction in the thickness direction having low output impedance has been presented in Ref. [7]. A strip electrode at the middle of the output part of the piezotransformer minimizes heat generation [8]. The main difference between traditional electromagnetic and piezoceramic transformers is in their small dimensions, weight and stray fields [1–4] and in their high efficiency [7–9]. The importance of the study as well as the reason for choosing ceramic materials for the piezoelectric transformers have been described in, for example, Refs. [3,4,7–11].

In Ref. [12] the forced vibrations of a classical Rosen-type transverse–longitudinal piezotransformer were analyzed and more precise formulae for transform ratio with regard to difference of the elastic compliance in the input and output sections were derived. It is well established that a transforming ratio is inversely proportional to the square frequency [13]. This fact explains why an operation of the planar transformers at higher modes of vibrations is impossible. The longitudinal mechanical stresses in input and output sections of the transformer were considered in Ref. [14] and it was shown that stresses in both sections are axisymmetric with respect to the separating line that is a good match with experimental data.

In the present paper the results of Refs. [12–14] are used for the analysis of the displacements, stresses, transforming ratio and input admittance of the transverse–longitudinal transformer with respect to dependence of the transformer parameters upon the difference of the elastic compliance in different sections as well as the influence of the electrostatic state of an output section. The frequency properties and the stress state of a rectangular piezoceramic transformer are also analyzed. Satisfactory matching of the calculated results and experimental data is observed. As far as possible IRE Standard notation [15] will be used in this article.

2. Basic relations for the electroelastic vibrations of a transverse–longitudinal piezotransformer

A classic Rosen-type planar monolithic piezotransformer consists of an exciting (input) section of length l_1 with transverse polarization and a generating (output) section of length l_2 with longitudinal polarization. The plate thickness is $2h$ and width is $2b$. There are very thin silver electrodes at the upper and lower surfaces of an input section and at an edge of the output section, and preliminary polarization throughout the thickness. The generating (output) section has a single very thin silver electrode at an edge and almost uniform polarization along the length. A one-dimensional approximation is used because the width $2b$ is much smaller than length $(l_1 + l_2)$. The variables in the first and second sections are marked as "1" and "2" respectively.

The physical processes in a plate planar piezotransformer may be explained as follows. The applied voltage V_1 from an external generator draws a current I_1 in an exciting section and excites the electromechanical vibrations in a device due to an inverse piezoelectric effect. In order to excite the intensive electroelastic vibrations in a plate, the frequency of the electric voltage V_1 is selected to be equal to the resonant frequency. The mechanical deformations of an output section due to the direct piezoelectric effect induce a piezoelectric charge Q_2, an electric voltage V_2 and an electric current I_2 at its electrode. The derivation of basic relations for the forced electroelastic vibrations of a transverse–longitudinal piezotransformer was made in Ref. [12]. The variables with index "1" have transverse orientation and the variables with index "2" have longitudinal orientation.

The expressions for the components of the mechanical displacements U_1, U_2 and stresses σ_1, σ_2 are

$$U_1 = \frac{[d_{31}E_1\varDelta - Ak_1\sin(k_1l_1)]\sin(k_1y) + Ak_1\cos(k_1l_1)\cos(k_1y)}{k_1\varDelta\cos(k_1l_1)}, \tag{1}$$

$$\sigma_1 = \frac{[d_{31}E_1\varDelta - Ak_1\sin(k_1l_1)]\cos(k_1y)}{\varDelta s_{11}^E\cos(k_1l_1)} - \frac{Ak_1\sin(k_1y) + d_{31}E_1\varDelta}{s_{11}^E\varDelta}, \tag{2}$$

$$U_2 = \frac{[g_{33}D_2\varDelta + Ak_2\sin(k_2l_2)]\sin(k_2y) + Ak_2\cos(k_2l_2)\cos(k_2y)}{k_2\varDelta\cos(k_2l_2)}, \tag{3}$$

$$\sigma_2 = \frac{[g_{33}D_2\varDelta + Ak_2\sin(k_2l_2)]\cos(k_2y)}{s_{33}^D\varDelta\cos(k_2l_2)} - \frac{Ak_2\sin(k_2y) + g_{33}D_2\varDelta}{s_{33}^D\varDelta}. \tag{4}$$

Here $k_1^2 = \rho\omega^2 s_{11}^E$, $k_2^2 = \rho\omega^2 s_{33}^D$, $k_1l_1 = x$ is the undimensional frequency, ρ is density, ω is the angular frequency, d_{31}, g_{33} are the piezoelectric constants [15], s_{11}^E, s_{33}^D are the elastic compliance constants at constant electric field E and constant electric displacement D, respectively, E_1 and D_2 are the electric field tension and electric displacement (induction) in sections, y is the longitudinal co-ordinate.

Note that

$$k_2l_2 = tx, \quad y/l_1 = L, \quad k_1y = Lx, \quad k_2y = Ltx, \quad \delta = l_1/l_2 \tag{5}$$

and then

$$A = s_{33}^D d_{31}E_1d_1\cos(tx) - s_{11}^E g_{33}D_2d_2\cos(x), \quad \varDelta = s_{11}^E k_2\varDelta_*, \tag{6}$$

$$d_1 = 1 - \cos(x), \quad d_2 = 1 - \cos(tx), \quad \varDelta_* = \cos(x)\sin(tx) + t\delta\sin(x)\cos(tx). \tag{7}$$

At the resonant frequencies $\varDelta_* \equiv 0$ and the terms U_i and σ_i become infinite. To avoid such results the mechanical losses are introduced by a mechanical quality Q_m as in Refs. [2,12–14,16]:

$$x = x_1 - \mathrm{j}x_2 = x_1\left(1 - \frac{1}{Q_m}\right). \tag{8}$$

The components of the mechanical displacements and stresses in a plate are complex functions of a complex variable x and may be rewritten as

$$U_1 = \frac{d_{31}E_1 l_1}{x} \frac{[\Delta_* \sin(Lx) + tA_* \cos(x + Lx)]}{\Delta_* \cos(x)}, \tag{9}$$

$$\sigma_1 = \frac{d_{31}E_1}{s_{11}^E} \frac{\Delta_*[\cos(Lx) - \cos(x)] - tA_* \sin(x + Lx)}{\Delta_* \cos(x)}, \tag{10}$$

$$U_2 = \frac{d_{31}E_1 l_1}{x} \frac{[q\Delta_* \sin(Ltx) + t^2 A_* \cos(tx + Ltx)]}{t\Delta_* \cos(tx)}, \tag{11}$$

$$\sigma_2 = \frac{d_{31}E_1}{s_{11}^E} \frac{q\Delta_*[\cos(Ltx) - \cos(tx)] - t^2 A_* \sin(tx + Ltx)}{t^2 \Delta_* \cos(tx)}, \tag{12}$$

where

$$A_* = d_1 \cos(tx) - \frac{q}{t^2} d_2 \cos(x) \tag{13}$$

and

$$\mathrm{q} = \frac{g_{33}D_2}{d_{31}E_1} \tag{14}$$

is an unknown influence factor which characterizes an influence of the electric displacement D_2 on the input section. The functions d_1, d_2, A_* and Δ_* are complex also and

$$\Delta_* = \Delta_1 + \mathrm{j}\Delta_2, \tag{15}$$

$$\Delta_1 = \cos(x_1)\sin(tx_1) + t\delta \sin(x_1)\cos(tx_1), \tag{16}$$

$$\Delta_2 = (1 + t^2\delta)x_2 \sin(x_1)\sin(tx_1) - (1 + \delta)tx_2 \cos(x_1)\cos(tx_1). \tag{17}$$

In deriving (16), (17) the hyperbolic expressions of the trigonometric functions of imaginary argument were used and it was assumed that $\sinh(x_2) \cong x_2, \cosh(x_2) \cong 1$. The terms proportional to $(x_2)^2$ as well as the products of small quantities were omitted. After these re-formations at the resonant frequencies $\Delta_1 \equiv 0$ but $\Delta_2 \neq 0$ and all mechanical components are finite.

For a piezoceramic transformer relations (9)–(12) are fundamental. They may be used for studying the electroelastic vibrations of the piezotransformer and for investigating its frequency and electromechanical properties.

3. An electric behaviour of a piezotransformer

The electric current in the input section of a piezotransformer is determined as the first derivative of the total piezocharge Q_1 with respect to time, which under a harmonic law of variation in the variables may be written as [12]

$$
\begin{aligned}
I_1 &= \mathrm{j}\omega Q_1 = \mathrm{j}\omega \int_{s1} D_1\,\mathrm{d}s = 2\mathrm{j}\omega b\varepsilon_{33}^T \int_{-l1}^{0}\left(E_1 + \frac{d_{31}\sigma_1}{\varepsilon_{33}^T}\right)\mathrm{d}y \\
&= -\mathrm{j}\omega C_{01}^s V_1 - \mathrm{j}\omega C_{01}^T \frac{k_{31}^2\tan(x)}{x} + \mathrm{j}\omega \frac{C_{01}^T V_1 k_{31}^2 s_{33}^D d_1^2\cos(tx)}{l_1 \Delta\cos(x)} - \mathrm{j}\omega \frac{2bd_{31}d_{33}D_2 d_1 d_2}{\varepsilon_{33}^T \Delta}. \qquad (18)
\end{aligned}
$$

Here ε_{33}^T is the permittivity when the stress is constant or zero [15] and

$$
C_{01}^T = \frac{2bl_1\varepsilon_{33}^T}{2h}, \quad C_{01}^s = (1-k_{31}^2)C_{01}^T, \quad k_{31}^2 = \frac{d_{31}^2}{s_{11}^E\varepsilon_{33}^T}, \quad V_1 = -2E_{x1}h, \quad g_{33} = \frac{d_{33}}{\varepsilon_{33}^T}. \qquad (19)
$$

The voltage V_2 is induced at the output of the generating sections, it is equal to [12]

$$
V_2 = -\int_0^{l2} E_2\,\mathrm{d}y = -\beta_{33}^T D_2 l_2\left(1 + k_D^2 - \frac{k_D^2\tan(tx)}{tx}\right) + \frac{g_{33}^2 s_{11}^E D_2 d_2^2\cos(x)}{s_{33}^D \Delta\cos(tx)} + \frac{g_{33}d_{31}V_1 d_1 d_2}{2h\Delta}, \qquad (20)
$$

where [17]

$$
k_{33}^2 = \frac{d_{33}^2}{s_{33}^E\varepsilon_{33}^T}, \quad k_D^2 = \frac{g_{33}^2}{s_{33}^D\beta_{33}^T}, \quad \beta_{33}^T = \frac{1}{\varepsilon_{33}^T}. \qquad (21)
$$

An input admittance of a piezotransformer is determined as a ratio of an input current I_1 to input voltage V_1, hence

$$
Y_1 = \frac{I_1}{V_1} = -\mathrm{j}\omega C_{01}^T\left[1 - k_{31}^2 + k_{31}^2\frac{\tan(x)}{x}\right] + \mathrm{j}\omega C_{01}^T \frac{k_{31}^2 s_{33}^D d_1^2\cos(tx)}{l_1\Delta\cos(x)} + \mathrm{j}\omega\frac{2bd_{31}d_{33}D_2 d_1 d_2}{\Delta\varepsilon_{33}^T V_1}. \qquad (22)
$$

The ratio of output voltage V_2 to input voltage V_1 is a transformation ratio of a piezotransformer and may be found from Eq. (20) as

$$
K_{21} = \frac{V_2}{V_1} = \frac{\beta_{33}^T D_2 l_2}{V_1}\left[1 + k_D^2 - k_D^2\frac{\tan(tx)}{(tx)}\right] + \frac{g_{33}^2 s_{11}^E D_2 d_2^2\cos(x)}{V_1 s_{33}^D\Delta\cos(tx)} + \frac{g_{33}d_{31}d_1 d_2}{2h\Delta}. \qquad (23)
$$

Relations (18), (20), (22) and (23) are very common because no assumptions on the electrical conditions of the piezotransformer have yet been made. These formulae may be used to analyze how the input and output sections influence each other.

Accounting for formulae (7), (14) and (21) relations (22) and (23) may be rewritten in a more simple form as

$$
Y_1 = -\mathrm{j}\omega C_{01}^T\left[b_{11} - \frac{k_{31}^2 t d_1^2\cos(tx)}{\delta x\Delta_*\cos(x)} + q\frac{k_{31}^2 d_1 d_2}{\delta t\Delta_*}\right], \qquad (24)
$$

$$
K_{21} = \frac{qd_{31}}{d_{33}}\left[b_{21} - \frac{k_D^2 d_2^2\cos(x)}{(tx)\Delta_*\cos(tx)}\right]\frac{l_1}{2h} + \frac{d_{31}d_{33}d_1 d_2}{s_{11}^E\varepsilon_{33}^T(tx)\Delta_*}\frac{l_1}{2h}, \qquad (25)
$$

where

$$
b_{11} = 1 - k_{31}^2 + \frac{k_{31}^2\tan(x)}{x}, \quad b_{21} = 1 + k_D^2 - \frac{k_D^2\tan(tx)}{(tx)}. \qquad (26)
$$

Under a no-load case, which characterizes the possibilities of the piezotransformer, it is customary to consider that electrostatic induction at the output section is equal to zero. $D_2 = 0$, and hence an influence factor q must be equal to zero too. In such a case expressions (24) and (25) may be simplified to

$$Y_{10} = -\mathrm{j}\omega C_{01}^{T}\left[b_{11} - \frac{k_{31}^2 t d_1^2 \cos(tx)}{\delta x \Delta_* \cos(x)}\right], \tag{27}$$

$$K_{210} = \frac{d_{31} d_{33} d_1 d_2}{s_{11}^{E} \varepsilon_{33}^{T} (tx) \Delta_*} \frac{l_1}{2h}. \tag{28}$$

Formulae (25) and (28) for the transformation ratio have real and imaginary parts. At the resonant frequencies $\Delta_1 \equiv 0$ and $\Delta_* = \mathrm{j}\Delta_2$, therefore

$$K_{21res} = -\frac{\mathrm{j}l_1}{2h}\frac{d_{33}d_{31}}{s_{11}^{E}\varepsilon_{33}^{T}}\frac{2Q_m}{(\delta x_1)(tx_1)}\frac{d_{10}d_{20}}{\Delta_{20}}, \tag{29}$$

where

$$d_{10} = 1 - \cos(x_1),\ \ d_{20} = 1 - \cos(tx_1),$$
$$\Delta_{20} = (1 + t^2\delta)\sin(x_1)\sin(tx_1) - (1+\delta)t\cos(x_1)\cos(tx_1). \tag{30}$$

Formula (29) shows that the resonant transformation ratio is directly proportional to product $d_{10}d_{20}$ and inversely proportional to squared frequency $(x_1)^2$. The absolute value of the resonant transformation ratio (29) may be written as

$$|K_{21}|_{res} = \frac{l_1}{2h}\frac{d_{33}|d_{31}|}{s_{11}^{E}\varepsilon_{33}^{T}}\frac{2Q_m}{\delta t (x_1)^2}\frac{|d_{10}d_{20}|}{|\Delta_{20}|}. \tag{31}$$

This formula explains why calculated data for the first and second modes are approximately equal. The fact is that the product $(d_{10}d_{20})$ for TsTStBS-2 ceramics is equal 0.92 at a first resonance and 3.85 at a second while $(x_1)_2/(x_1)_1 = 2$, hence relation $d_{10}d_{20}/(x_1)^2$ approximately remains for the first two modes. For the third mode product $(d_{10}d_{20})$ decreases to 0.93 while $(x_1)_3/(x_1)_1 = 3$, and the calculated transformation ratio decreases by more than 9 times. The relation $d_{10}d_{20}/(x_1)_4^2$ approaches zero for the forth mode. The transformation ratio for higher overtones of longitudinal vibrations became less than 1/9 of that for the first mode and device operation is not good enough.

Formulae (29) and (31) may be simplified by reformation of Eq. (16) and (30). Such approximate relations may be written as

$$\Delta_1 = \sin(tx_1)\cos(x_1) + t\delta\sin(x_1)\cos(tx_1) \cong \sin(tx_1)\cos(x_1) + \sin(x_1)\cos(tx_1) = \sin[(1+t)x_1] \tag{32}$$

and

$$\Delta_{20} = (1+t^2\delta)\left[\sin(x_1)\sin(tx_1) - \frac{(1+\delta)t}{(1+t^2\delta)}\cos(x_1)\cos(tx_1)\right]$$
$$\cong 2t[\sin(x_1)\sin(tx_1) - \cos(x_1)\cos(tx_1)] = 2t\cos[(1+t)x_1] \tag{33}$$

since

$$\frac{(1+\delta)t}{(1+t^2\delta)} = \mu \cong 1. \tag{34}$$

Real piezotransformers have such length that $\delta \approx 1$ and for $1 \geqslant t \geqslant 0.7$ a ratio μ differs from 1.0 less than 6%. Following this the resonant frequencies may be found from the approximate formula

$$\sin[(1+t)x_1] = 0, \quad x_1 \cong \frac{n\pi}{(1+t)} \quad (n = 1, 2, 3, \ldots). \tag{35}$$

At these frequencies

$$\Delta_{20} = 2t\cos\left[(1+t)\frac{n\pi}{(1+t)}\right] = 2t\cos(n\pi) = \pm 2t \tag{36}$$

and resonant transforming ratio is

$$|K_{21}|_{res} = \frac{l_1}{2h}\frac{d_{33}|d_{31}|}{s_{11}^E \varepsilon_{33}^T}\frac{2Q_m(1+t)^2\eta_0}{2t^2(n\pi)^2}, \tag{37}$$

where

$$\eta_0 = \left[1-\cos\left(\frac{n\pi}{1+t}\right)\right]\left[1-\cos\left(\frac{tn\pi}{1+t}\right)\right] = 4\sin^2\left(\frac{n\pi}{1+t}\right)\sin^2\left(\frac{tn\pi}{1+t}\right) \quad (n = 1, 2, 3, \ldots). \tag{38}$$

For a no-load operation and the principal longitudinal resonance in Ref. [2] the following formula was derived:

$$K_{u0} = \frac{4Q_m}{\pi^2}\frac{d_{33}d_{31}Y_3^E}{\varepsilon_{33}^E(1-k_{33}^2)}\frac{L}{a}. \tag{39}$$

Here Y_3^E is Young's modulus of an output section, L is the half-length, a is the thickness, and the following assumption is made:

$$\frac{Y_3^E}{Y_1^E} = \frac{s_{11}^E}{s_{33}^E} \approx 1. \tag{40}$$

If in Eq. (37) $n = t = 1$, then

$$|K_{21}|_1 = \frac{4Q_m}{\pi^2}\frac{d_{33}d_{31}}{s_{11}^E\varepsilon_{33}^T}\frac{l_1}{2h}, \tag{41}$$

which completely coincides with Eq. (39), since $Y_3^E/(1-k_{33}^2) = 1/s_{33}^D$, and the difference between s_{33}^D and S_{11}^E are not taken into account in Ref. [2].

Formulae (29), (31) and (37) may be applied only at the resonant frequencies. The next complex expression may be used for any frequencies

$$K_{21} = \frac{l_1}{2h}\frac{d_{31}d_{33}}{s_{11}^E\varepsilon_{33}^T}(a_{211} - ja_{212}), \tag{42}$$

where

$$a_{21} = a_{211} - ja_{212} \tag{43}$$

is a complex amplitude–frequency transfer function, the real and imaginary parts of which are equal to

$$a_{211} = \frac{(d + 2x_2 b)\Delta_1}{tx_1(\Delta_1^2 + \Delta_2^2)}, \quad a_{212} = \frac{d\Delta_2}{tx_1(\Delta_1^2 + \Delta_2^2)} \tag{44}$$

and

$$d = d_{10}d_{20}, \quad b = td_{10}b_1 + d_{20}b_2,$$

$$b_1 = \sin\left(\frac{tx_1}{2}\right)\cos\left(\frac{tx_1}{2}\right), \quad b_2 = \sin\left(\frac{x_1}{2}\right)\cos\left(\frac{x_1}{2}\right). \tag{45}$$

The transformation ratio (42) may be regarded in the common case as a product of three factors

$$K_{21} = l_0 d_0 a_{21} \quad (l_0 = l_1/2h, d_0 = d_{31}d_{33}/S_{11}^E \varepsilon_{33}^T). \tag{46}$$

The first factor l_0 is a ratio of the plate geometrical dimensions, i.e. a half-length l_1 to thickness $2h$. The second factor d_0 is determined by material constants of the piezoceramics and may be increased by choosing better chemical compositions [4,9,10]. Also the third factor is a complex amplitude–frequency transfer function a_{21}. Its magnitude is in proportion to the product of trigonometric factor d and mechanical quality $Q_{\rm m}$.

One may calculate, for example, values of factor d_0 for two types of piezoceramics. Material constants for the barium titanate ceramics are taken from Ref. [2] as

$$d_{33} = 1.61 \times 10^{-10}\ \mathrm{m/V}, \quad d_{31} = -0.73 \times 10^{-10}\ \mathrm{m/V},$$

$$\varepsilon_{33}^T = 1.44 \times 10^{-8}\ \mathrm{F/m}, \quad Y_3^E = 9.5 \times 10^{10}\ \mathrm{N/m^2}, \quad k_{33}^2 = 0.1$$

and for TsTStBS-2 piezoceramics one has [17] $d_{33} = 330 \times 10^{-12}$ C/N, $d_{31} = -160 \times 10^{-12}$ C/N, $s_{11}^E = 12.5 \times 10^{-12}\ \mathrm{m^2/N}$, $\varepsilon_{33}^T/\varepsilon_0 = 2100$, $\varepsilon_0 = 8.85 \times 10^{-12}$ F/m.

Substituting these data in Eq. (46) gives $|d_0| = 0.086$ for the barium titanate ceramics and $|d_0| = 0.227$ for TsTStBS-2 piezoceramics.

4. Numerical results

All calculations for this paper were made in complex form and the data for TsTStBS-2 ceramics were used for plate dimensions $80 \times 18 \times 2$ mm, i.e. $l_1/2h = 20$, $(l_1 + l_2)/2b = 4.44$. After substituting these parameters in Eq. (9) the results were plotted in Figs. 1 and 2 for $t = 0.8$, $V_1 = 10$ V, $Q_m = 100$. The figure notations U11, U21 and U31 are displacements in the first section at first, second and third longitudinal modes respectively, V_1 is input voltage and $E_1 = V_1/2h$. Displacement amplitudes are very small and they decrease with increase of frequency. The displacement distributions in the output section are the same but they have the opposite sign.

Numerical results for elastic stresses are demonstrated at Figs. 3 and 4. The figure notations T1, T2 are the stresses in the first section of the plate at the first and second longitudinal modes of

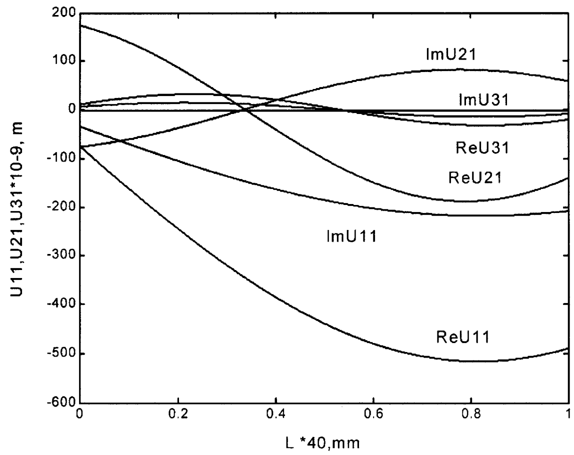

Fig. 1. Distributions of real and imaginary parts of the elastic displacements U11, U21 and U31 for first three longitudinal modes of input section.

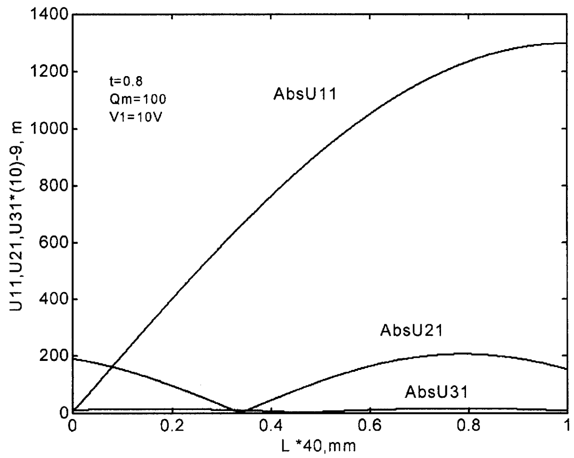

Fig. 2. Distributions of absolute values of elastic displacements for first three longitudinal modes of the input section.

vibration respectively. The amplitude of mechanical stresses at the third longitudinal mode is very small and may not be plotted on the same figure.

Fig. 5 shows the frequency dependence of the functions $f_1 = 2t\cos[(1+t)x_1]$, $f_2 = \sin[(1+t)x_1]$, $z_1 = \Delta_1$ in a range $0 \leqslant x_1 \leqslant 14$ for $t = 0.8$ and $q = 0$. The zeros of the function z_1, which correspond to the resonant frequencies of the piezotransformer, almost coincide with the zeros of the simplified function f_2. Hence the resonant frequencies may be determined by formula (35). The function $\Delta_1 \equiv 0$ equals zero at the resonant frequencies and $\Delta_2 \cong f_1$. The maxima of this function correspond to resonant frequencies.

Fig. 6 demonstrates a marked difference between zeros of the functions $z_{11} = \Delta_1$ $(t = 0.8)$ and $z_{12} = \Delta_1$ $(t = 1)$. The fact is that a replacement of formula (35) by approximate relation $x_1 = n\pi/2$ is not correct if $t \neq 1$.

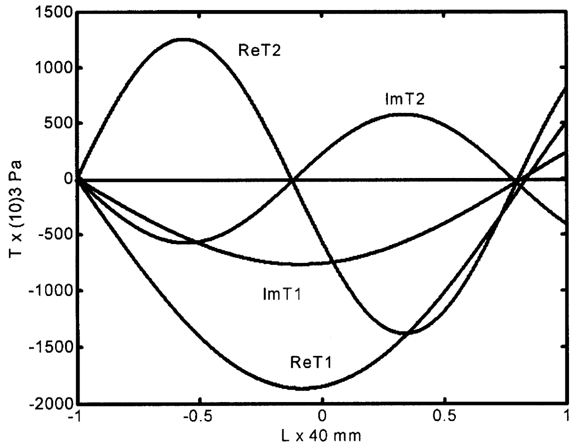

Fig. 3. Distributions of real and imaginary parts of elastic stresses for first two longitudinal modes of plate piezotransformer for $t = 0.8$, $Q_m = 100$ and $V1 = 10$ V.

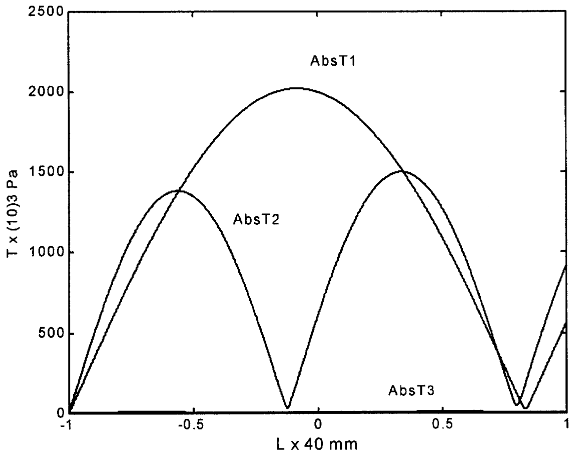

Fig. 4. Distributions of absolute values of elastic stresses for first three longitudinal modes of the plate piezotransformer.

5. Comparison with an experiment

The experimental investigations were carried out on several models of piezotransformers of transverse–longitudinal type. Copper silvered wires with a diameter of 0.1 mm were soldered to the surface plate electrodes and used to connect to the circuit. Vibrations were excited by a variable voltage from a generator in a range from 20 to 200 kHz. The output section of the piezotransformer was connected to an electronic digital voltmeter and the electronic digital frequency meter controlled the operative frequency. Table 1 presents the characteristic frequencies f_m and f_n in kHz and their corresponding maximum and minimum admittances Y in mS m for the first eight registered modes of vibrations of a planar piezotransformer with dimensions 80 ×

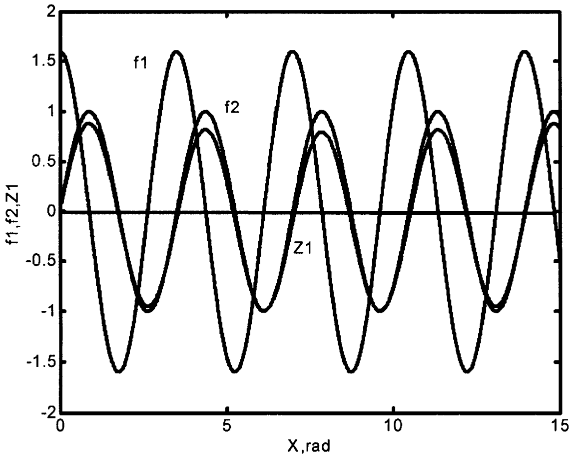

Fig. 5. The graphs of the functions $f_1 = 2t\cos[(1+t)x_1]$, $f_2 = \sin[(1+t)x_1]$, $z_1 = \Delta_1$.

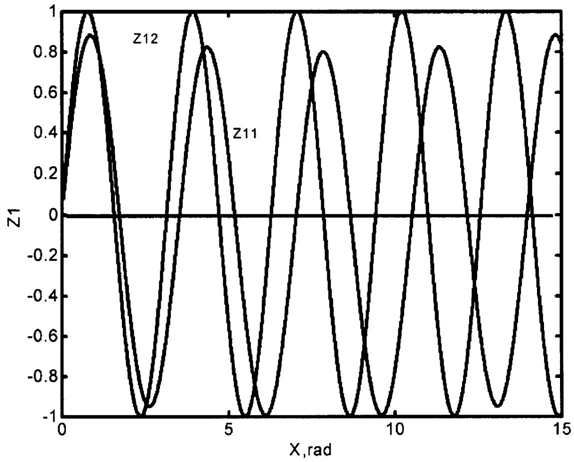

Fig. 6. The graphs of the function Δ_1 for $t = 0.8$ (Z11) and $t = 1$ (Z12).

Table 1
Characteristic frequencies and admittances for first eight modes of a piezotransformer

f_m (kHz)	21.31	42.29	61.90	81.66	92.38	96.04	99.37	136.3
f_n (kHz)	21.69	42.88	62.07	81.85	93.19	98.19	100.2	137.2
Y_m (mS m)	19	20.8	7.41	14.5	41.1	95.8	28.4	34.1
Y_n (mS m)	0.095	0.24	1.76	3.23	3.53	1.18	0.56	1.02

18×2 mm from PKD ceramics. The following values for maxima of an output potential were obtained (the frequencies in kHz is in the numerator and the transformation ratio is in the denominator): 21.23/256, 42.01/342, 61.81/118, 86.35/14.9, 93.05/18, 96.78/15.1, 99.33/18 and 136.51/113.

The first two modes are almost equal in maximum admittance and transformation ratio, the third and fourth modes are much weaker, and the 96.04 kHz mode is of the greatest intensity and its admittance exceeds that of the first mode five times. On the other hand the intensive 93.05, 96.78 and 99.33 kHz modes induce at the output electrodes a much smaller voltage than do the first two modes. The 81.66 kHz resonance is not detected from the output voltage but the new 86.35 kHz mode, which is absent in Table 1 and about whose deformation nothing can be said, is observed. The graph of Fig. 7 was obtained, when an input section of a piezotransformer was connected with a sweep generator IChX-300 between its input and output sockets as a rejecting circuit. A sweep generator IChX-300 had 135 Ω input and output impedance. The greater the input admittance of a piezoelectric plate, the deeper a rejecting downfall in the graph. The marks L1–L6 on the graph relate to the longitudinal modes, T1–T3 denote the intensive lateral modes and E1 is an edge mode. The length–width ratio for the testing transformer is 80:18 = 4.44. Many years ago the author investigated the planar vibrations of a thin rectangular piezoceramic plate with various length–width ratios in the interval $1 \leqslant a/b \leqslant 8$. The results for a range $2 \leqslant a/b \leqslant 4$ were published in author's doctoral thesis (1976) but the rest of results remain unpublished. The characteristics of a piezotransformer are now compared with those of a rectangular plate.

Fig. 8 demonstrates the amplitude–frequency dependence for such a plate with $a/b = 4.5$. Both amplitude and frequency are presented in Figs. 7 and 8 in relative units, because a device screen had such a view. It is easy to establish that the amplitude–frequency characteristics are similar for a rectangular piezoceramic plate and for a plate piezoceramic transformer. Their main difference is that the piezoplate spectrum is more rigid than it is for a piezotransformer with the same geometric dimensions. The even numbers of longitudinal modes L2 and L6 for rectangular plates are absent.

Fig. 9 shows the frequency dependencies of the output voltage for the first and second vibration modes. The graphs were plotted in a single figure for two frequency intervals 20–23 and 40–43 kHz. The transformation ratios (the numerator) and quality factors (the denominator) were the following [13]: 54/163 and 72/221. The self-capacity of the piezotransformer was 4.75 times

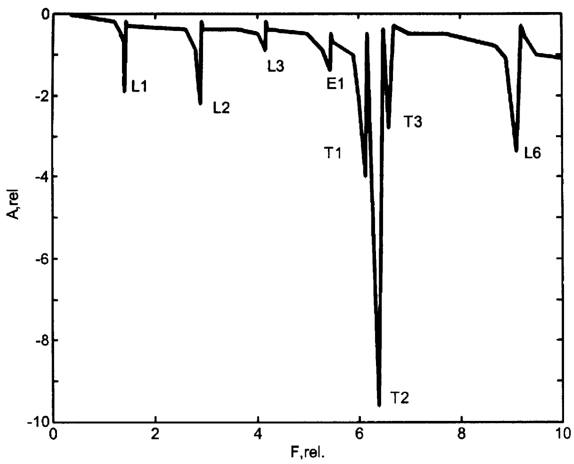

Fig. 7. Dependence of amplitude A_{rel} on frequency F_{rel} for PKD piezotransformer with $a/b = 4.44$.

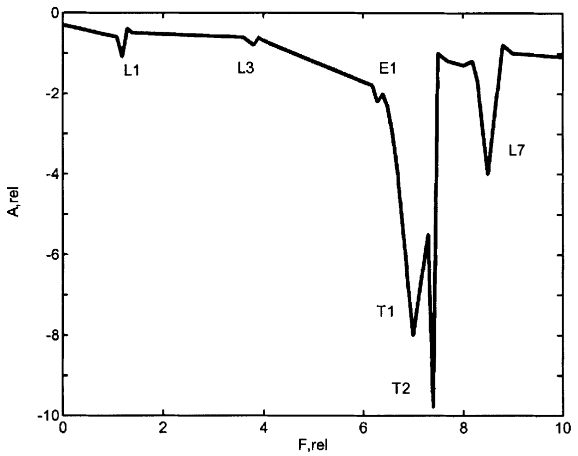

Fig. 8. Dependence of amplitude A_{rel} on frequency F_{rel} for TsTS-19 rectangular plate with $a/b = 4.5$.

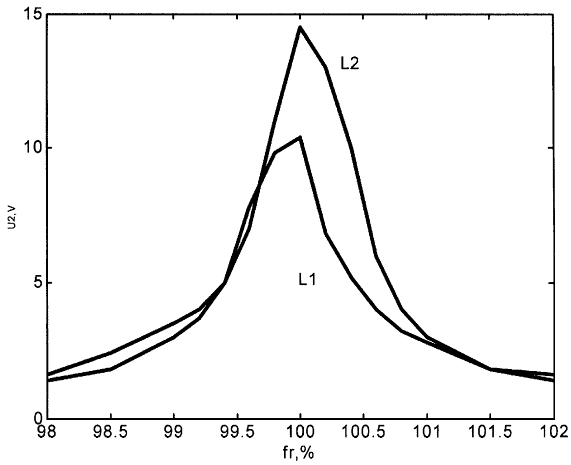

Fig. 9. The output voltage frequency dependence at first and second modes [13].

less than the total measuring circuit capacity. It means that the actual transformation ratios were 256 and 342, which is a good match with the theoretical values.

The levels of the dynamic stresses in an exciting section and their distribution along the axis were studied by the piezotransformer-transducer method [18,19]. Twelve piezotransformer transducers of 3.1 mm in diameter were divided (separated) in the electrode coating in the middle of the input section. Their centres were located almost uniformly [14] along the longitudinal co-ordinate. Each separate electrode may be regarded as a piezoelectric transformer exit. The potentials V_t of such transducers are proportional to the mechanical stresses in the plate under them so that the stress distribution fits the distribution of the potentials.

The transfer ratios $K = V_t/V_0$ (V_0 is input potential) for the piezotransformer transducers are shown in Fig. 10 for the first four experimental modes (n is transducer number). L1, L2 and L3

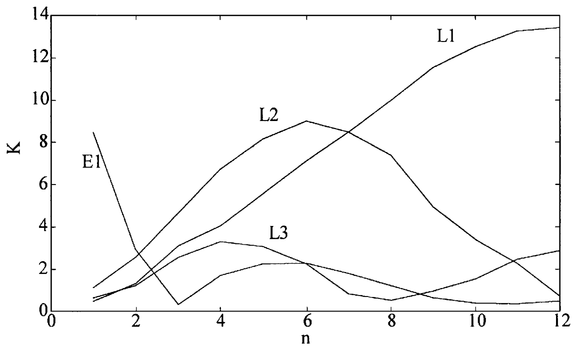

Fig. 10. The distribution of the piezotransformer transducer potentials in an exciting section.

denote the first three longitudinal modes whereas the fourth mode behaves completely differently. The dynamic stresses on it are commensurable with the stresses of the third mode everywhere except at the end, where they sharply increase and approach the maximum stresses of the first mode. This peculiar mode may be identified with the edge resonance [20]. Being weak, this mode is characterized by a sharp increase in the amplitude of the displacements near the plate corners and that of the stresses near its ends. An edge mode is not detected from output potential difference and is marked on the graph by E1. The distributions of the dynamic stresses for an input section are a good match with numerical results as was shown in Figs. 3 and 4. It should be noted here that the voltmeter in the method of the piezotransformer transducer [18,19] shows only an absolute value of the measured potential. The phase of measured potential remains unknown. For this reason distributions for modes L2 and L3 in Fig. 10 do not have negative parts.

6. Conclusions

The refined formula of the transformation ratio for a planar piezotransformer of the transverse–longitudinal type is re-formed and discussed. It is shown that the transformation ratio near resonant frequencies is directly proportional to piezoelectric moduli and inversely proportional to frequency squared. The transformation ratios at the first and second modes of vibrations for all piezoceramics are almost equal to one another as well as for the third and sixth modes.

Operation of the planar piezotransformer at the high frequencies is not acceptable.

The one-dimensional rod model adequately describes the first six longitudinal modes of a piezotransformer.

The dynamic stresses are axisymmetric about the boundary line and equal in amplitude at the corresponding points of the input and output sections.

It is established by an experimental analysis that the amplitude–frequency characteristics are similar for a rectangular piezoceramic plate and for a plate piezoceramic transformer but the piezoplate spectrum is more rigid than it is for a piezotransformer with the same geometric dimensions.

Satisfactory matching of the calculated results and experimental data is observed.

Acknowledgements

The author would like to thank Prof. N.A. Shul'ga for his support of this work and guidance.

References

[1] US Patent 439 992 1954 / Rosen C.A.- 29.06.1954.
[2] H.W. Katz (Ed.), *Solid State Magnetic and Piezoelectric Devices*, Wiley, New York, 1959.
[3] V.V. Lavrinenko, *Piezoelectric Transformers*, Energiya, Moscow, 1975 (in Russian).
[4] E.G. Smazhevskaya, R.A. Zhuchina, N.A. Podol'ner, The problem of the influence of the basic parameters of a piezoceramic material on the characteristics of experimental models of piezotransformers, in: *Transmitters and Receivers of Ultrasonic Vibrations* Part 2, LDNTP, 1966, pp. 22–35 (in Russian).
[5] E.C. Munk, The equivalent electrical circuit for radial modes of piezoelectric ceramic disk with concentric electrodes, *Philips Research Reports* 20 (1965) 170–189.
[6] G.G. Zaretskiy-Feoktistov, Vibrations of a thin piezoceramic disk, *Soviet Applied Mechanics* 20 (9) (1984) 832–836.
[7] M. Yamamoto, Y. Sasaki, A. Ochi, T. Inoue, S. Hamamura, Step-down piezoelectric transformer for AC-DC converters, *Japanese Journal of Applied Physics* 1.40 (5B) (2001) 3637–3642.
[8] Y. Fuda, K. Kumasaka, M. Katsumo, H. Sato, Y. Ino, Piezoelectric transformer for cold cathode fluorescent lamp inverter, *Japanese Journal of Applied Physics* 1.36 (5B) (1997) 3050–3052.
[9] O. Ise, K. Saton, Y. Mamiya, High power characteristics of piezoelectric ceramics in Pb(Mn1/3Nb2/3)O3-PbTiO3 system, *Japanese Journal of Applied Physics* 1.38 (9B) (1999) 5531–5534.
[10] A.A. Yerofeyev, G.A. Danov, V.N. Frolov, *The Piezoceramic Transformers and Their Application in Radioelectronics*, Radio i Svyaz, Moscow, 1988 (in Russian).
[11] T. Inoue, M. Yamamoto, S. Kawashima, S. Hirose, Third order longitudional piezoelectric ceramic transformer for high-voltage power inverter, *IEICE Transactions on Electronics* E81 (7) (1998) 1128–1135.
[12] V.L. Karlash, The forced electroelastic vibrations of a planar piezoelectric transformer of longitudinal-transverse type, *International Applied Mechanics* 36 (7) (2000) 923–930.
[13] V.L. Karlash, Frequency properties of a planar piezoelectric transformer of longitudinal-transverse type, *International Applied Mechanics* 36 (8) (2000) 1103–1111.
[14] V.L. Karlash, The stress state of rectangular piezoceramic plate with transverse–longitudinal polarization, *International Applied Mechanics* 37 (3) (2001) 386–392.
[15] IRE Standards on Piezoelectric Crystals: Measurements of Piezoelectric Ceramics, *Proceedings of the IRE* 49 (1961) 1161–1169.
[16] R. Holland, Representation of dielectric, elastic and piezoelectric losses by complex coefficients, *Journal of the Acoustical Society of America* 42 (6) (1967) 1223–1231.
[17] N.A. Shul'ga, A.M. Bolkisev, *The Vibrations of Piezoelectric Bodies*, Naukova Dumka, Kiev, 1990 (in Russian).
[18] V.L. Karlash, A.T. Ulitko, About one method of an investigation of radial vibrations of thin Piezoceramic plate, *Dopovidi Akademii Nauk Ukrains'koi RSR, Seriya A* (9) (1974) 804–807 (in Ukrainian).
[19] V.L. Karlash, A.T. Ulitko, A method of an investigation of the mechanical stresses in the vibrating piezoceramic bodies, *Electrichestvo* (11) (1976) 82–83.
[20] V.T. Grinchenko, V.L. Karlash, V.V. Meleshko, A.T. Ulitko, Analysis of the planar vibrations of rectangular piezoceramic plates, *Prikladna Mekhanika* 12 (5) (1976) 71–78.